

Novel 1,2,4-Thiadiazole Derivatives as Potent Neuroprotectors: Approach to Creation of Bioavailable Drugs

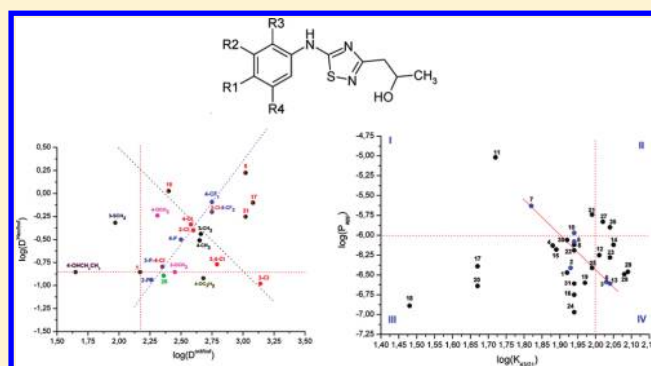
German L. Perlovich,^{*,†,‡} Alexey N. Proshin,[‡] Tatyana V. Volkova,[†] Ludmila N. Petrova,[‡] and Sergey O. Bachurin[‡]

[†]Institute of Solution Chemistry, Russian Academy of Sciences, 153045 Ivanovo, Russia

[‡]Institute of Physiologically Active Compounds, Russian Academy of Sciences, 142432 Chernogolovka, Russia

ABSTRACT: Novel 1,2,4-thiadiazole derivatives as potent neuroprotectors were synthesized and identified. Their ability to inhibit the glutamate stimulated Ca uptake was measured. Permeation experiments on the phospholipid membranes were conducted, and the apparent permeability coefficients were obtained. The partition coefficients in *n*-octanol/buffer (pH 7.4) and *n*-hexane/buffer (pH 7.4) immiscible phases (as model systems for characterizing gastrointestinal tract membranes and BBB) were determined. A classification of the studied compounds from the standpoint of “permeability–activity” properties was proposed.

KEYWORDS: 1,2,4-thiadiazole derivatives, neuroprotectors, permeability, phospholipid membrane, partitioning, specific activity



1. INTRODUCTION

The *N*-methyl-D-aspartate (NMDA) receptor belongs to a family of the ionotropic glutamate receptors and performs important functions in the central nervous system. It is mainly involved in the neuronal signaling processes, memory consolidation, and synaptic plasticity.^{1,2} The neurotoxicity which is induced by NMDA hyperactivation leads to a number of pathological conditions, ranging from acute neurodegenerative disorders, such as stroke and trauma, to chronic forms of neurodegenerative diseases, i.e., Huntington's disease, Parkinson's disease, Alzheimer's disease (AD), as well as lateral amyotrophic sclerosis.^{3–6}

It is generally recognized that the specific inhibition of calcium ion influx via hyperactivated glutamate (Glu)-receptor-channel complex (GluR), particularly NMDA-subtype receptor, provides sufficient protection against a diverse group of neurological stresses related to the Glu excitotoxicity, such as brain ischemia, AD, etc.⁷ In the case of AD, it is considered that specific inhibitors of Glu-stimulated calcium uptake in nervous cells provide sufficient neuronal protection against the neurotoxic effect associated with β -amyloid peptide ($A\beta$) as the major pathogen in AD, which is particularly realized by the potentiating of endogenous glutamate excitotoxic effects.⁸ On the other hand, it is assumed that glutamate receptor agonists (especially α -amino-3-hydroxy-5-methyl-4-isoxazolepropionic acid (AMPA)-subtype receptor agonists) exhibit strong cognition-enhancing effects due to the activation of glutamatergic neurotransmission.⁹ Such dualism in properties of glutamatergic compounds explains a strong interest in these compounds as promising neuroprotectors and cognition-enhancers.

The interaction with target receptors is a key property in the designing of drug molecules. However, the drug delivery processes also play an important role in the creation of bioavailable drugs. Therefore, obtaining the screening parameters characterizing solubility, partitioning, and membrane permeability is an essential part of drug design. In the present study, a variety of *in vitro* and *in vivo* methods were used to perform the primary screening and the selection of potential neuroprotectors in a wide spectrum of GluR-ligands. Particularly, the properties of novel 1,2,4-thiadiazoles (see Table 1 in the Experimental Section) were analyzed to inhibit the specific glutamate-stimulated calcium ions uptake (Glu-Ca-uptake) in rat brain synaptosomes. The noted compounds correspond to molecules which include a thiadiazole pharmacophoric fragment. This class of substances demonstrates very interesting pharmacological¹⁰ and neuroprotector¹¹ properties. Glutamate neuro-mediator plays an important role in the working of the nervous system. However, excess of the neuromediator leads to superactivation of the glutamate receptors and can generate programmed cell death (apoptosis).¹² The inhibition ability of $^{45}\text{Ca}^{2+}$ glutamate-dependent uptake in rat brain synaptosomes gives an opportunity to estimate the influence of the compounds on pathological processes at various neurodegenerative diseases.^{13,14}

Received: January 8, 2012

Revised: February 14, 2012

Accepted: February 20, 2012

Published: February 21, 2012

Table 1. Structures of Studied Compounds

| Compound | R | Compound | R | Compound | R | Compound | R |
|----------|---|----------|---|----------|---|----------|---|
| 1 | | 9 | | 17 | | 24 | |
| 2 | | 10 | | 18 | | 25 | |
| 3 | | 11 | | 19 | | 26 | |
| 4 | | 12 | | 20 | | 27 | |
| 5 | | 13 | | 21 | | 28 | |
| 6 | | 14 | | 22 | | 29 | |
| 7 | | 15 | | 23 | | 30 | |
| 8 | | 16 | | 31 | | | |

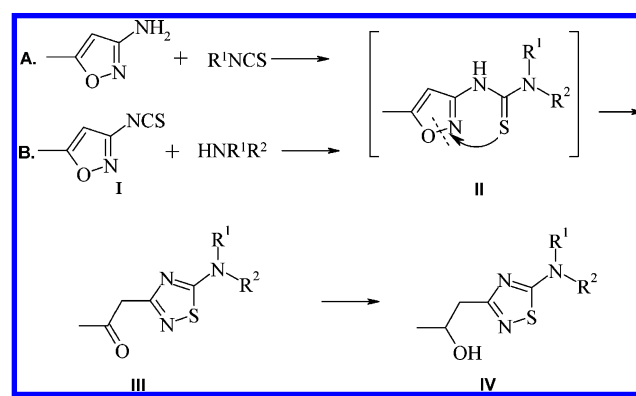
It should be noted that, for the considered class of the compounds, it keeps the Lipinski's rule of five. This fact confirms, once more, that selected 1,2,4-thiadiazoles could be perspective candidates as druglike substances. This study is aimed at developing a novel approach for the prediction of bioavailable drug molecules with maximal specific activity.

2. EXPERIMENTAL SECTION

2.1. Synthesis. **2.1.1. General Procedure for Preparing Novel 1,2,4-Thiadiazoles.** Synthetic approaches to novel 1,2,4-thiadiazoles were carried out according to Scheme 1.

The compounds synthesized are presented in Table 1. 1-[5-Amino-1,2,4-thiadiazol-3-yl]propan-2-ols (**IV**) were prepared by a reduction of appropriated 1-[5-amino-1,2,4-thiadiazol-3-yl]propan-2-ones (**III**). The synthetic method for ketones (**III**) is based on Boulton–Katritzky's rearrangement¹⁵ of isoxazolic thiourea (**II**) (obtained by a standard reaction between isothiocyanates and 3-amino-5-methyl-isoxazole (way A) in dipolar aprotic solvents (DMSO, acetonitrile) to 1,2,4-thiadiazoles). At room temperature the reaction in DMSO passes completely in 5–6 h.¹⁶ It should be mentioned that this method of synthesis makes it possible to produce only N-monosubstituted derivatives of 1,2,4-thiadiazole, namely [5-N-monosubstituted-amino-1,2,4-thiadiazol-3-yl]propan-2-ones (**III**, R² = H). Therefore, 3-isothiocyanato-5-methylisoxazole (**I**)¹⁷ was utilized to obtain N,N-disubstituted derivatives of 1,2,4-thiadiazole synthesized in

Scheme 1



the first instance. The received isothiocyanate was introduced in the reaction with secondary amines (way B) (inaccessible for this rearrangement before), and such an approach gave an opportunity for synthesizing the original N,N-disubstituted derivatives of 1,2,4-thiadiazoles (**III**) with the yield of 60–95%. Next, the keto-derivatives of thiadiazole (**III**) were reduced by sodium borohydride in methanol to afford the desirable 1-[5-amino-1,2,4-thiadiazol-3-yl]propan-2-ols (**IV**).¹⁸

2.1.2. Chemical Procedures. 1-[5-amino-1,2,4-thiadiazol-3-yl]propan-2-ols were synthesized by standard and accessible

methods at the Institute of Physiologically Active Compounds of the Russian Academy of Sciences.

3-Isothiocyanato-5-methylizoxazole (I). 3-Amino-5-methylizoxazole (49.05 g, 0.5 M) in CH_2Cl_2 (300 mL) was added dropwise to the stirred mixture of thiophosgene (42.2 mL, 0.55 M) and NaHCO_3 (92.4 g, 1.1 M) in H_2O (200 mL). The reaction mixture was cooled in an ice bath and kept under stirring for 1 h. After that the dichloromethane layer was separated and washed out with a saturated aqueous solution of NaCl (2×50 mL). The solution was dried (Na_2SO_4), and the solvent was evaporated. The obtained oil was distilled in vacuum. The yield amounted to 36.8 g (52.6%), bp 39–41 °C (1 mmHg). $^1\text{H NMR}$ [200 MHz, CDCl_3] δ : 2.50 (c, 3H, CH_3), 6.00 (c, 1H, CH). $^{13}\text{C NMR}$ [200 MHz, CDCl_3] δ : 172.9 (C_5), 153.1 (C_3), 145.4 (C_7), 100.1 (C_4), 13.2 (C_6).

2.1.3. General Procedure for the Preparation of (R,S)-1-[5-Amino-1,2,4-thiadiazol-3-yl]propan-2-ols (IV). Step 1. 3-Isothiocyanato-5-methylizoxazole (0.01 M) in CH_3CN (10 mL) was added slowly to the stirred solution of amine (0.01 M) in CH_3CN (10 mL). After the addition was over, the mixture was brought to reflux. Then the solution was cooled to room temperature. Generally, one day was required for precipitate formation. The grown crystals were filtered.

Step 2. 1-[5-Amino-1,2,4-thiadiazol-3-yl]propan-2-one (0.01 M) obtained at step 1 was dissolved in 20 mL of methanol. NaBH_4 (0.015 M) was added portionwise to the solution, and the mixture was stirred for 30 min, at the same time hydrogen gassing was stopped. The solvent was removed until the resultant residue was dry, and then the residue was taken up in dichloromethane/water. The organic layer was separated, dried over Na_2SO_4 , and filtered. The solvent was evaporated. The crude powder was recrystallized from isopropanol to derive the final product. The overall yield was 60–90%.

(R,S)-1-[(5-Phenylamino)-1,2,4-thiadiazol-3-yl]propan-2-ol (1). The overall yield for the two steps was 62%; mp 101–103 °C. $^1\text{H NMR}$ [200 MHz, CDCl_3] δ : 1.32 (3H, d, $J = 6.3$ Hz, CH_3), 2.85 (1H, dd, $J = 3.0, 15.5$ Hz, CH), 3.02 (1H, dd, $J = 8.8, 15.5$ Hz, CH), 4.10 (1H, br s, OH), 4.32 (m, 1H, CH), 7.15–7.52 (5H, m, ArH), 9.16 (1H, br s, NH). Anal. ($\text{C}_{11}\text{H}_{13}\text{N}_3\text{OS}$) $\text{C}_8\text{H}_7\text{N}$.

(R,S)-1-[5-(4-Methylphenylamino)-1,2,4-thiadiazol-3-yl]propan-2-ol (2). Yield 73%; mp 116–118 °C. $^1\text{H NMR}$ [200 MHz, $\text{DMSO}-d_6$] δ : 1.19 (3H, d, $J = 5.5$ Hz, CH_3), 2.33 (3H, s, CH_3), 2.73 (1H, dd, $J = 6.0, 13.7$ Hz, CH), 2.84 (1H, dd, $J = 7.0, 13.7$ Hz, CH), 4.17 (1H, m, CH), 4.41 (1H, d, $J = 4.5$ Hz, OH), 7.12 (2H, d, $J = 8.3$ Hz, ArH), 7.34 (2H, d, $J = 8.3$ Hz, ArH), 10.64 (1H, s, NH). Anal. ($\text{C}_{12}\text{H}_{15}\text{N}_3\text{OS}$) $\text{C}_8\text{H}_7\text{N}$.

(R,S)-1-[5-(4-Ethoxyphenylamino)-1,2,4-thiadiazol-3-yl]propan-2-ol (3). Yield 72%; mp 111–113 °C. $^1\text{H NMR}$ [200 MHz, CDCl_3] δ : 1.30 (3H, d, $J = 5.5$ Hz, CH_3), 1.48 (3H, t, $J = 7.0$ Hz, CH_3), 2.86 (2H, m, CH_2), 4.07 (2H, q, $J = 7.0$ Hz, CH_2), 4.27 (1H, m, CH), 4.30 (1H, br s, OH), 6.97 (2H, d, $J = 8.6$ Hz, ArH), 7.23 (2H, d, $J = 8.6$ Hz, ArH), 8.68 (1H, br s, NH). Anal. ($\text{C}_{13}\text{H}_{17}\text{N}_3\text{O}_2\text{S}$) $\text{C}_8\text{H}_7\text{N}$.

(R,S)-1-[5-(3-Chloro-4-fluorophenylamino)-1,2,4-thiadiazol-3-yl]propan-2-ol (4). Yield 68%; mp 124–126 °C. $^1\text{H NMR}$ [200 MHz, $\text{DMSO}-d_6$] δ : 1.18 (3H, d, $J = 6.3$ Hz, CH_3), 2.73 (1H, dd, $J = 6.3, 14.4$ Hz, CH), 2.87 (1H, dd, $J = 6.7, 14.4$ Hz, CH), 4.17 (1H, m, CH), 4.29 (1H, d, $J = 4.7$ Hz, OH), 7.20 (1H, t, $J = 8.8$ Hz, ArH), 7.45 (1H, ddd, $J = 2.8, 4.2, 9.1$ Hz, ArH), 7.82 (1H, dd, $J = 2.8, 6.5$ Hz, ArH), 8.98 (1H, br s, NH). Anal. ($\text{C}_{11}\text{H}_{11}\text{ClFN}_3\text{OS}$) $\text{C}_8\text{H}_7\text{N}$.

(R,S)-1-[5-(4-Chlorophenylamino)-1,2,4-thiadiazol-3-yl]propan-2-ol (5). Yield 83%; mp 132–134 °C. $^1\text{H NMR}$ [200 MHz, CDCl_3] δ : 1.33 (3H, d, $J = 6.2$ Hz, CH_3), 2.86 (1H, dd, $J = 3.0, 15.6$ Hz, CH), 3.04 (1H, dd, $J = 8.6, 15.6$ Hz, CH), 4.30 (1H, br s, OH), 4.31 (1H, m, CH), 7.24 (2H, d, $J = 8.9$ Hz, ArH), 7.43 (2H, d, $J = 8.5$ Hz, ArH), 8.42 (1H, br s, NH). Anal. ($\text{C}_{11}\text{H}_{12}\text{ClN}_3\text{OS}$) $\text{C}_8\text{H}_7\text{N}$.

(R,S)-1-[5-[4-(1-Hydroxyethyl)phenylamino]-1,2,4-thiadiazol-3-yl]propan-2-ol (6). Yield 64%; mp 144–146 °C. $^1\text{H NMR}$ [200 MHz, $\text{DMSO}-d_6$] δ : 1.14 (3H, d, $J = 6.0$ Hz, CH_3), 1.33 (3H, d, $J = 6.5$ Hz, CH_3), 2.66 (1H, dd, $J = 6.1, 14.2$ Hz, CH), 2.81 (1H, dd, $J = 7.0, 14.2$ Hz, CH), 4.13 (1H, m, CH), 4.42 (1H, d, $J = 4.4$ Hz, OH), 4.66 (1H, m, CH), 4.84 (1H, d, $J = 4.0$ Hz, OH), 7.27 (2H, d, $J = 8.4$ Hz, ArH), 7.38 (2H, d, $J = 8.4$ Hz, ArH), 10.66 (1H, s, NH). Anal. ($\text{C}_{13}\text{H}_{17}\text{N}_3\text{O}_2\text{S}$) $\text{C}_8\text{H}_7\text{N}$.

(R,S)-1-[5-(4-Trifluoromethylphenylamino)-1,2,4-thiadiazol-3-yl]propan-2-ol (7). Yield 85%; mp 143–145 °C. $^1\text{H NMR}$ [200 MHz, CDCl_3] δ : 1.35 (3H, d, $J = 6.3$ Hz, CH_3), 2.91 (1H, dd, $J = 8.6, 15.5$ Hz, CH), 3.08 (1H, dd, $J = 3.0, 15.5$ Hz, CH), 3.80 (1H, br s, OH), 4.36 (1H, m, CH), 7.39 (2H, d, $J = 8.6$ Hz, ArH), 7.70 (2H, d, $J = 8.6$ Hz, ArH), 9.30 (1H, br s, NH). Anal. ($\text{C}_{12}\text{H}_{12}\text{F}_3\text{N}_3\text{O}_2\text{S}$) $\text{C}_8\text{H}_7\text{N}$.

(R,S)-1-[5-(3-Chloro-4-methylphenylamino)-1,2,4-thiadiazol-3-yl]propan-2-ol (8). Yield 76%; mp 104–106 °C. $^1\text{H NMR}$ [200 MHz, CDCl_3] δ : 1.36 (3H, d, $J = 6.2$ Hz, CH_3), 2.43 (3H, s, CH_3), 2.88 (1H, dd, $J = 8.6, 15.5$ Hz, CH), 3.05 (1H, dd, $J = 3.0, 15.5$ Hz, CH), 4.35 (1H, m, CH), 4.51 (1H, br s, OH), 7.14 (1H, dd, $J = 2.4, 8.1$ Hz, ArH), 7.34 (2H, d, $J = 8.5$ Hz, ArH), 9.24 (1H, br s, NH). Anal. ($\text{C}_{12}\text{H}_{14}\text{ClN}_3\text{OS}$) $\text{C}_8\text{H}_7\text{N}$.

(R,S)-1-[5-(3,4-Dichlorophenylamino)-1,2,4-thiadiazol-3-yl]propan-2-ol (9). Yield 77%; mp 143–145 °C. $^1\text{H NMR}$ [200 MHz, CDCl_3] δ : 1.35 (3H, d, $J = 6.1$ Hz, CH_3), 2.88 (1H, dd, $J = 8.6, 15.6$ Hz, CH), 3.06 (1H, dd, $J = 2.8, 15.6$ Hz, CH), 4.35 (1H, m, CH), 4.45 (1H, s, OH), 7.18 (1H, dd, $J = 2.7, 8.6$ Hz, ArH), 7.48 (2H, m, ArH), 9.17 (1H, br s, NH). Anal. ($\text{C}_{11}\text{H}_{11}\text{Cl}_2\text{N}_3\text{OS}$) $\text{C}_8\text{H}_7\text{N}$.

(R,S)-1-[5-(4-Fluorophenylamino)-1,2,4-thiadiazol-3-yl]propan-2-ol (10). Yield 82%; mp 103–105 °C. $^1\text{H NMR}$ [200 MHz, $\text{DMSO}-d_6$] δ : 1.18 (3H, d, $J = 6.3$ Hz, CH_3), 2.72 (1H, dd, $J = 4.0, 14.2$ Hz, CH), 2.85 (1H, dd, $J = 7.0, 14.2$ Hz, CH), 4.17 (1H, m, CH), 4.35 (1H, d, $J = 4.4$ Hz, OH), 7.06 (2H, t, $J = 8.3$ Hz, ArH), 7.55 (2H, ddd, $J = 2.38, 4.6, 9.1$ Hz, ArH), 10.69 (1H, s, NH). Anal. ($\text{C}_{11}\text{H}_{12}\text{FN}_3\text{OS}$) $\text{C}_8\text{H}_7\text{N}$.

(R,S)-1-[5-(2-Chloro-5-trifluoromethylphenylamino)-1,2,4-thiadiazol-3-yl]propan-2-ol (11). Yield 66%; mp 116–118 °C. $^1\text{H NMR}$ [200 MHz, CDCl_3] δ : 1.36 (3H, d, $J = 6.2$ Hz, CH_3), 2.94 (1H, dd, $J = 8.4, 15.6$ Hz, CH), 3.09 (1H, dd, $J = 3.5, 15.6$ Hz, CH), 3.61 (1H, br s, OH), 4.36 (1H, m, CH), 7.37 (1H, dd, $J = 1.2, 8.3$ Hz, ArH), 7.61 (1H, d, $J = 8.0$ Hz, ArH), 8.26 (1H, s, ArH), 8.31 (1H, br s, NH). Anal. ($\text{C}_{12}\text{H}_{11}\text{ClF}_3\text{N}_3\text{OS}$) $\text{C}_8\text{H}_7\text{N}$.

(R,S)-1-[5-(3-Methylphenylamino)-1,2,4-thiadiazol-3-yl]propan-2-ol (12). Yield 72%; mp 88–89 °C. $^1\text{H NMR}$ [200 MHz, $\text{DMSO}-d_6$] δ : 1.18 (3H, d, $J = 6.2$ Hz, CH_3), 2.37 (3H, s, CH_3), 2.72 (1H, dd, $J = 6.2, 14.2$ Hz, CH), 2.84 (1H, dd, $J = 7.0, 14.2$ Hz, CH), 4.17 (1H, m, CH), 4.46 (1H, d, $J = 4.4$ Hz, OH), 7.12 (2H, d, $J = 6.8$ Hz, ArH), 7.14–7.30 (3H, m, ArH), 10.71 (1H, s, NH). Anal. ($\text{C}_{12}\text{H}_{15}\text{N}_3\text{OS}$) $\text{C}_8\text{H}_7\text{N}$.

(R,S)-1-[5-(4-Methoxyphenylamino)-1,2,4-thiadiazol-3-yl]propan-2-ol (13). Yield 81%; mp 90–91 °C. $^1\text{H NMR}$ [200 MHz, $\text{DMSO}-d_6$] δ : 1.18 (3H, d, $J = 6.3$ Hz, CH_3), 2.69 (1H, dd, $J = 7.0, 14.2$ Hz, CH), 2.82 (1H, dd, $J = 7.0, 14.2$ Hz, CH), 3.78 (3H, s, CH_3), 4.15 (1H, m, CH), 4.42 (1H, d, $J = 4.5$ Hz, OH),

6.87 (2H, d, $J = 9.0$ Hz, ArH), 7.40 (2H, d, $J = 9.0$ Hz, ArH), 10.54 (1H, s, NH). Anal. (C₁₂H₁₅N₃O₂S) C₁₂H₁₅N₃O₂S.

(*R,S*)-1-[5-(2-Chlorophenylamino)-1,2,4-thiadiazol-3-yl]propan-2-ol (**14**). Yield 77%; mp 86–88 °C. ¹H NMR [200 MHz, CDCl₃] δ : 1.36 (3H, d, $J = 6.1$, CH₃), 2.91 (1H, dd, $J = 8.8$, 15.6 Hz, CH), 3.08 (1H, dd, $J = 3.1$, 15.6 Hz, CH), 4.30 (1H, br s, OH), 4.34 (1H, m, CH), 7.15 (1H, t, $J = 7.5$ Hz, ArH), 7.35–7.55 (2H, m, ArH), 7.67 (1H, d, $J = 8.1$ Hz, ArH), 8.25 (1H, br s, NH). Anal. (C₁₁H₁₂ClN₃OS) C₁₁H₁₂ClN₃OS.

(*R,S*)-1-[5-(2-Fluorophenylamino)-1,2,4-thiadiazol-3-yl]propan-2-ol (**15**). Yield 73%; mp 79–81 °C. ¹H NMR [200 MHz, CDCl₃] δ : 1.34 (3H, d, $J = 6.1$, CH₃), 2.86 (1H, dd, $J = 8.6$, 15.7 Hz, CH), 3.03 (1H, dd, $J = 2.8$, 15.7 Hz, CH), 4.30 (1H, br s, OH), 4.33 (1H, m, CH), 7.20–7.48 (4H, m, ArH), 8.28 (1H, br s, NH). Anal. (C₁₁H₁₂FN₃OS) C₁₁H₁₂FN₃OS.

(*R,S*)-1-[5-(3-Methylthiophenylamino)-1,2,4-thiadiazol-3-yl]propan-2-ol (**16**). Yield 69%; mp 101–102 °C. ¹H NMR [200 MHz, CDCl₃] δ : 1.32 (3H, d, $J = 6.2$, CH₃), 2.53 (3H, s, CH₃), 2.83 (1H, dd, $J = 8.6$, 15.5 Hz, CH), 3.00 (1H, dd, $J = 2.9$, 15.5 Hz, CH), 4.28 (1H, br s, OH), 4.33 (1H, m, CH), 6.98–7.42 (4H, m, ArH), 8.35 (1H, br s, NH). Anal. (C₁₂H₁₅N₃O₂S₂) C₁₂H₁₅N₃O₂S₂.

(*R,S*)-1-[5-(3-Methyl-4-chlorophenylamino)-1,2,4-thiadiazol-3-yl]propan-2-ol (**17**). Yield 80%; mp 134–136 °C. ¹H NMR [200 MHz, DMSO-*d*₆] δ : 1.18 (3H, d, $J = 6.0$ Hz, CH₃), 2.34 (3H, s, CH₃), 2.73 (1H, dd, $J = 6.3$, 14.2 Hz, CH), 2.86 (1H, dd, $J = 6.7$, 14.2 Hz, CH), 4.16 (1H, m, CH), 4.44 (1H, d, $J = 4.7$ Hz, OH), 7.21 (1H, d, $J = 8.4$ Hz, ArH), 7.31 (1H, dd, $J = 2.3$, 8.3 Hz, ArH), 7.63 (1H, d, $J = 2.1$ Hz, ArH), 10.80 (1H, br s, NH). Anal. (C₁₂H₁₄ClN₃OS) C₁₂H₁₄ClN₃OS.

(*R,S*)-1-[5-(2-Methyl-3-chlorophenylamino)-1,2,4-thiadiazol-3-yl]propan-2-ol (**18**). Yield 71%; mp 124–125 °C. ¹H NMR [200 MHz, DMSO-*d*₆] δ : 1.17 (3H, d, $J = 6.0$ Hz, CH₃), 2.37 (3H, s, CH₃), 2.68 (1H, dd, $J = 6.0$, 14.1 Hz, CH), 2.80 (1H, dd, $J = 6.8$, 14.1 Hz, CH), 4.12 (1H, m, CH), 4.36 (1H, d, $J = 4.5$ Hz, OH), 7.17 (2H, m, ArH), 7.77 (1H, m, ArH), 10.08 (1H, br s, NH). Anal. (C₁₂H₁₄ClN₃OS) C₁₂H₁₄ClN₃OS.

(*R,S*)-1-[5-(3-Methoxyphenylamino)-1,2,4-thiadiazol-3-yl]propan-2-ol (**19**). Yield 69%; mp 123–124 °C. ¹H NMR [200 MHz, CDCl₃] δ : 1.20 (3H, d, $J = 6.3$, CH₃), 2.75 (1H, dd, $J = 8.6$, 15.6 Hz, CH), 2.94 (1H, dd, $J = 3.1$, 15.6 Hz, CH), 3.60 (1H, br s, OH), 3.74 (3H, s, CH₃), 4.19 (1H, m, CH), 6.55–6.77 (3H, m, ArH), 7.15–7.25 (3H, m, ArH), 8.96 (1H, br s, NH). Anal. (C₁₂H₁₅N₃O₂S) C₁₂H₁₅N₃O₂S.

(*R,S*)-1-[5-(3-Chlorophenylamino)-1,2,4-thiadiazol-3-yl]propan-2-ol (**20**). Yield 73%; mp 115–117 °C. ¹H NMR [200 MHz, CDCl₃] δ : 1.34 (3H, d, $J = 6.2$, CH₃), 2.87 (1H, dd, $J = 6.2$, 15.5 Hz, CH), 3.05 (1H, dd, $J = 3.0$, 15.5 Hz, CH), 4.20 (1H, br s, OH), 4.31 (1H, m, CH), 7.12–7.44 (4H, m, ArH), 8.59 (1H, br s, NH). Anal. (C₁₁H₁₂ClN₃OS) C₁₁H₁₂ClN₃OS.

(*R,S*)-1-[5-(Dibenzylamino)-1,2,4-thiadiazol-3-yl]propan-2-ol (**21**). Yield 77%; mp 65–66 °C. ¹H NMR [200 MHz, DMSO-*d*₆] δ : 1.18 (3H, d, $J = 6.1$ Hz, CH₃), 2.68 (1H, dd, $J = 6.7$, 14.1 Hz, CH), 2.80 (1H, dd, $J = 6.8$, 14.1 Hz, CH), 4.14 (1H, m, CH), 4.39 (1H, d, $J = 4.4$ Hz, OH), 4.65 (4H, s, N(CH₂)₂), 7.22–7.40 (10H, m, ArH). Anal. (C₁₉H₂₁N₃OS) C₁₉H₂₁N₃OS.

(*R,S*)-1-[5-(Cyclopropylamino)-1,2,4-thiadiazol-3-yl]propan-2-ol (**22**). Yield 67%; mp 121–123 °C. ¹H NMR [200 MHz, DMSO-*d*₆] δ : 0.59–0.84 (4H, m, (CH₂)₂), 1.13 (3H, d, $J = 6.6$ Hz, CH₃), 2.52 (1H, m, CH), 2.62 (1H, dd, $J = 6.0$, 14.2 Hz, CH), 2.71 (1H, dd, $J = 6.7$, 14.2 Hz, CH), 4.03 (1H, m, CH),

4.41 (1H, d, $J = 4.2$ Hz, OH), 8.65 (1H, s, NH). Anal. (C₈H₁₃N₃OS) C₈H₁₃N₃OS.

(*R,S*)-1-[5-(4-Pyridin-2-ylpiperazin-1-yl)-1,2,4-thiadiazol-3-yl]propan-2-ol (**23**). Yield 63%; mp 106–107 °C. ¹H NMR [200 MHz, DMSO-*d*₆] δ : 1.14 (3H, d, $J = 6.0$ Hz, CH₃), 2.63 (1H, dd, $J = 6.3$, 14.4 Hz, CH), 2.74 (1H, dd, $J = 7.0$, 14.4 Hz, CH), 3.60 (4H, m, N(CH₂)₂), 3.68 (4H, m, N(CH₂)₂), 4.08 (1H, m, CH), 4.31 (1H, d, $J = 4.4$ Hz, OH), 6.61 (1H, dd, $J = 4.9$, 7.9 Hz, PyH), 6.80 (1H, d, PyH), 7.50 (1H, td, $J = 7.9$, 2.0 Hz, PyH), 6.61 (1H, dd, $J = 2.1$, 4.9 Hz, PyH). Anal. (C₁₆H₁₉F₃N₄OS) C₁₆H₁₉F₃N₄OS.

(*R,S*)-1-[5-[4-(3-Trifluoromethylphenyl)piperazin-1-yl]-1,2,4-thiadiazol-3-yl]propan-2-ol (**24**). Yield 66%; mp 95–97 °C. ¹H NMR [200 MHz, DMSO-*d*₆] δ : 1.16 (3H, d, $J = 6.1$ Hz, CH₃), 2.65 (1H, dd, $J = 6.0$, 14.3 Hz, CH), 2.77 (1H, dd, $J = 6.8$, 14.3 Hz, CH), 3.42 (4H, m, N(CH₂)₂), 3.68 (4H, m, N(CH₂)₂), 4.12 (1H, m, CH), 4.32 (1H, d, $J = 4.4$ Hz, OH), 7.02–7.26 (4H, m, ArH). Anal. (C₁₆H₁₉F₃N₄OS) C₁₆H₁₉F₃N₄OS.

(*R,S*)-1-[3-(2-Hydroxypropyl)-[1,2,4]thiadiazol-5-yl]piperidine-4-carboxylic Acid Amide (**25**). Yield 60%; mp 134–136 °C. ¹H NMR [200 MHz, DMSO-*d*₆] δ : 1.12 (3H, d, $J = 6.1$ Hz, CH₃), 1.15–1.93 (4H, m, CH₂CHCH₂), 2.40 (1H, m, CH₂CHCH₂), 2.58 (1H, dd, $J = 6.0$, 14.4 Hz, CH), 2.70 (1H, dd, $J = 7.2$, 14.4 Hz, CH), 3.11–3.30 (2H, m, N(CH₂)₂), 3.75–3.92 (2H, m, N(CH₂)₂), 4.07 (1H, m, CH), 4.31 (1H, d, $J = 4.4$ Hz, OH), 6.60 (1H, br s, NH), 7.17 (1H, br s, NH). Anal. (C₁₁H₁₈N₄O₂S) C₁₁H₁₈N₄O₂S.

(*R,S*)-1-[5-(5-Methylisoxazol-3-ylamino)-[1,2,4]thiadiazol-3-yl]propan-2-ol (**26**). Yield 62%; mp 189–191 °C. ¹H NMR [200 MHz, DMSO-*d*₆] δ : 1.15 (3H, d, $J = 6.0$ Hz, CH₃), 2.41 (3H, s, CH₃), 2.73 (1H, dd, $J = 6.0$, 14.1 Hz, CH), 2.85 (1H, dd, $J = 7.0$, 14.1 Hz, CH), 4.12 (1H, m, CH), 5.70 (2H, br s, OH, NH), 6.01 (1H, s, CH). Anal. (C₉H₁₂N₄O₂S) C₉H₁₂N₄O₂S.

(*R,S*)-1-[5-[4-(4-Nitrophenyl)piperazin-1-yl]-1,2,4-thiadiazol-3-yl]propan-2-ol (**27**). Yield 74%; mp 91–93 °C. ¹H NMR [200 MHz, CDCl₃] δ : 1.31 (3H, d, $J = 6.3$ Hz, CH₃), 2.79 (1H, dd, $J = 8.9$, 15.6 Hz, CH), 2.98 (1H, dd, $J = 2.8$, 15.6 Hz, CH), 3.58–3.81 (8H, m, N(CH₂)₂N), 4.13 (1H, s, OH), 4.24 (1H, m, CH), 6.92 (2H, d, $J = 9.5$ Hz, ArH), 8.21 (2H, d, $J = 9.5$ Hz, ArH). Anal. (C₁₅H₁₉N₅O₃S) C₁₅H₁₉N₅O₃S.

(*R,S*)-1-[5-(6-Methylpyridin-2-ylamino)-[1,2,4]thiadiazol-3-yl]propan-2-ol (**28**). Yield 65%; mp 146–148 °C. ¹H NMR [200 MHz, DMSO-*d*₆] δ : 1.16 (3H, d, $J = 6.0$ Hz, CH₃), 2.74 (1H, dd, $J = 5.8$, 14.2 Hz, CH), 2.85 (1H, dd, $J = 6.8$, 14.2 Hz, CH), 4.14 (1H, m, CH), 4.45 (1H, d, $J = 4.2$ Hz, OH), 6.78 (1H, d, $J = 7.4$ Hz, PyH), 6.93 (1H, d, $J = 8.4$ Hz, PyH), 7.57 (1H, t, $J = 7.5$ Hz, PyH), 11.84 (1H, s, NH). Anal. (C₁₁H₁₄N₄OS) C₁₁H₁₄N₄OS.

(*R,S*)-1-[5-[2-(5-Methoxy-1H-indol-3-yl)ethylamino]-[1,2,4]thiadiazol-3-yl]propan-2-ol (**29**). Yield 66%; mp 116–118 °C. ¹H NMR [200 MHz, DMSO-*d*₆] δ : 1.17 (3H, d, $J = 6.1$ Hz, CH₃), 2.64 (1H, dd, $J = 5.8$, 14.5 Hz, CH), 2.73 (1H, dd, $J = 7.0$, 14.5 Hz, CH), 3.03 (2H, t, $J = 6.9$ Hz, CH₂), 3.58 (2H, q, $J = 6.7$ Hz, CH₂), 3.82 (3H, s, CH₃), 4.11 (1H, m, CH), 4.42 (1H, br s, OH), 6.69 (1H, dd, $J = 2.3$, 8.6 Hz, ArH), 6.97 (1H, d, $J = 2.1$ Hz, ArH), 7.07 (1H, d, $J = 2.1$ Hz, ArH), 7.22 (1H, d, $J = 2.1$ Hz, ArH), 8.31 (1H, t, NH), 10.50 (1H, s, NH). Anal. (C₁₆H₂₀N₄O₂S) C₁₆H₂₀N₄O₂S.

(*R,S*)-N-[3-(2-Hydroxypropyl)-[1,2,4]thiadiazol-5-yl]benzamide (**30**). Yield 69%; mp 73–75 °C. ¹H NMR [200 MHz, D₂O] δ : 1.23 (3H, d, $J = 6.3$ Hz, CH₃), 2.89–2.97 (2H, m, CH₂), 4.35 (1H, m, CH), 7.45–7.60 (3H, m, ArH), 8.05–8.15 (2H, m, ArH). Anal. (C₁₂H₁₃N₃O₂S) C₁₂H₁₃N₃O₂S.

(*R,S*)-1-[5-(2-Methyl-5-chlorophenylamino)-[1,2,4]-thiadiazol-3-yl]propan-2-ol (**31**). Yield 81%; mp 102–103 °C. ¹H NMR [200 MHz, DMSO-*d*₆] δ: 1.26 (3H, d, *J* = 6.2 Hz, CH₃), 2.30 (s, 3H, CH₃), 2.79 (1H, dd, *J* = 8.6, 15.5 Hz, CH), 2.95 (1H, dd, *J* = 2.2, 15.5 Hz, CH), 4.14 (s, 1H, OH), 4.25 (m, 1H, CH), 7.13 (1H, dd, *J* = 1.8, 8.1 Hz, ArH), 7.22 (1H, d, *J* = 8.1 Hz, ArH), 7.44 (1H, d, *J* = 1.8 Hz, ArH), 8.60 (s, 1H, NH). Anal. (C₁₂H₁₄ClN₃OS) C, H, N.

2.2. Materials and Solvents. 1-Octanol (*n*-octanol, CH₃(CH₂)₇OH, MW 130.2, lot 11K3688) ARG was from Sigma Chemical Co. (USA). *n*-Hexane (C₆H₁₄, MW 86.18, lot 07059903 C) ARG was from SDS (Peypin, France).

Phosphate buffer solution (pH 7.4) was prepared by mixing the solutions of appropriate phosphoric acid sodium and potassium salts. All the chemicals were AR grade. The pH values were measured by the use of a Toledo MP 220 pH meter (Mettler, USA) standardized with pH 1.68 and 9.22 solutions.

Egg phosphatidyl choline, Lipoid E-80 was obtained from Lipoid (Germany). Culture inserts (Transwell-Clear, *d* = 6.5 mm) and plates were purchased from Corning Inc. Corning, USA, filters in existence were removed, and mixed cellulose ester filters (0.65 μm pore size) from Millipore, Billerica, USA were fused on. Phospholipid vesicle-based barriers were prepared according to the procedure described earlier.¹⁹

2.3. Permeation Studies. Stock solutions of the compounds under study (2.5 × 10⁻⁵ to 2.5 × 10⁻³ mol·L⁻¹) were prepared by dissolving the drug in phosphate buffer solution pH 7.4. Containing KH₂PO₄, Na₂HPO₄·12H₂O, NaCl, NaN₃, and water, the solution was adjusted to pH 7.4 with HCl/NaOH if necessary. Concentrations of different drug solutions were chosen on the assumption of analytical considerations as well as for obtaining the sink conditions during permeation studies. The concentrations of different drug solutions had to be high enough for the obtainment of a definite amount of a drug in an acceptor chamber during permeation studies to be quantified by means of UV-absorbance and still be below the solubility limit.

The method of the liposome preparation involves film hydration/filter extrusion. Egg phosphatidyl choline (1.8 g) was dissolved in a mixture of chloroform and methanol (2:1) (6 mL) in a round-bottom flask. The organic solvent was removed under vacuum at 55 °C. The deposited lipid film was exposed to vacuum of 55 hPa at room temperature for an additional period of 3 h to remove traces of solvent, before hydration with phosphate buffer, containing 10% (v/v) ethanol to obtain a 6% (w/v) liposomal dispersion. The liposome dispersion was then filter-extruded through 0.8 and 0.4 μm polycarbonate membrane filters (Millipore) at room temperature. The extrusion was done by hand with a syringe through the filters in a 25 mm Swinnex Filter Holder from Millipore. To obtain liposomes of two different sizes, one portion was extruded five times through the 0.8 μm polycarbonate membrane filter while another portion was extruded five additional passages through filters with 0.4 μm pore size.

Permeation studies were performed after loading the inserts (the facility for bearing the 0.65 μm pore size mixed cellulose ester filter) with drug solution (100 μL) and placing them into separate acceptor compartments containing phosphate buffer solution (600 μL) (pH 7.4). The permeation experiment was carried out at room temperature without agitation, and inserts were moved to wells containing equal quantities of fresh buffer solution. Taking into account the low solubility of the compounds under investigation, the operational range of 12–24 h

was optimal. In conclusion of the permeation experiment, samples (200 μL) from each acceptor compartment were transferred into 96-well UV 96-well black plates (Costar) and drug concentrations were measured spectrophotometrically (Spectramax 190; Molecular devices, Molecular Devices Corporation, California, USA) at the most appropriate wavelength for each drug. A blank well was filled with pure phosphate buffer pH 7.4. The electrical resistance of the lipid barriers was measured (Millicell-ERS, Millipore, USA) immediately after completion of permeation studies. To find out the resistance of the lipid barrier itself, a value of 119 Ω resulting from the filter characteristics was subtracted from the observed resistance meaning. Such a difference was then multiplied by the surface area (0.33 cm²) to be normalized for the dimensions of the insert. The experiments were performed at least in triplicate with three inserts in each parallel for every compound. The mean values and standard deviations are reported.

The standard time dependences of the cumulative amount of permeated drug consisted of 6–9 points, and every point represented the mean value of three parallels. The *r*²-meanings were always higher than 0.99. Repeatability corresponded to 3.9–20.1%, and an intermediate precision of 2.7–29.4% was observed for different drugs using such a novel method.

The linear part of the slope of the curve of the standard time dependence of the cumulative amount represented the steady-state flux rate. If a lag time was observed before the steady-state conditions were attained, and the saturation conditions took place at the end of the experiments, only the middle points of the cumulative plot were used for the calculation procedure, based on the steady-state flux. The obtained flux rates were used to calculate the apparent permeability coefficient (*P*_{app}, cm·s⁻¹) by means of the following equation:

$$P_{app} = J / (A \cdot (C_d - C_a)) \quad (1)$$

where *J* is the observed flux rate at steady-state (nmol·s⁻¹), *A* is the surface area of the insert (cm²), and *C*_{*d*} and *C*_{*a*} are the concentrations of the solutions in the donor and acceptor chambers (nmol/mL), respectively. The experiments were performed under the sink conditions; that is, the drug concentration in the acceptor chamber did not exceed 10% of the drug concentration in the donor chamber at any time.²⁰

2.4. Determination of Partition Coefficients. The isothermal saturation method was used to determine the partition coefficients in *n*-octanol/buffer (pH 7.4), *D*^{oct/buf}, and *n*-hexane/buffer (pH 7.4), *D*^{hex/buf}, systems. All the experiments were carried out at 25 °C. The substance concentrations were measured spectrophotometrically using calibration curves. The partition coefficient was calculated using the following equation:

$$D = C_{ow} / C_{wo} \quad (2)$$

where *C*_{ow} and *C*_{wo} are the molar concentrations of solute in the mutually saturated phases of octanol and water. The accuracy of the *D* value was verified by checking the mass balance of the starting amount of compound *i* compared to the total amount of the compound partitioned between the two phases:

$$m_i = m_{ow} + m_{wo} \quad (3)$$

where *m*_{*i*} = *C*_{*i*}*V*_{*i*} is the starting mass (in moles) of the compound, *m*_{ow} = *C*_{ow}*V*_{ow} is the mass of the substance dissolved in the water-saturated octanol phase, and *m*_{wo} = *C*_{wo}*V*_{wo} is the mass of the substance dissolved in the octanol-saturated water phase.

2.5. Calcium-Blocking Property Experiments. Interaction between the compounds and the glutamate-dependent calcium uptake system was studied on newborn (8–11 days old) rat brain synaptosomal P₂-fraction isolated according to the following method: synaptosomes were suspended in incubation buffer A (132 mM NaCl, 5 mM KCl, 5 mM HEPES) pH 7.4 stored at 0 °C during the experimental stage. The aliquots of synaptosomes (50 μL) were transposed to buffer A containing test compound and ⁴⁵Ca-samples. Calcium ion uptake was stimulated by introducing the glutamate solution (200 μM). After 5 min incubation at 37 °C, the process was terminated by the filtration on GF/B-filters. The sample was washed three times with cold buffer B (145 mM KCl, 10 mM Tris, 5 mM Trilon B) followed by radioactivity measuring with scintillator counter SL-4000 Intertechinc.

In preliminary experiments, all the compounds were tested for the ability to inhibit glutamate stimulated Ca uptake at the concentration of 100 μM. If the inhibition of Glu-Ca-uptake was 50% and more, then further studies were carried out to determine the concentration dependence of inhibition and the corresponding value of $K_{43/21}$ was measured according to the following equation:

$$K_{43/21} = 100[(Ca_4 - Ca_3)/(Ca_2 - Ca_1)] \quad (4)$$

where Ca_1 is the the Ca^{2+} influx in the blank experiment (without glutamate and test compounds); Ca_2 is the Ca^{2+} influx in the presence of glutamate only (Glu-Ca-uptake); Ca_3 is the Ca^{2+} influx in the presence of test compound (without glutamate); and Ca_4 is the Ca^{2+} influx in the presence of both glutamate and test compound.

2.6. Calculation Procedure. All the descriptors were calculated with the program package HYBOT-PLUS (version of 2003) in Windows.²¹ Structural similarity was estimated using Tanimoto similarity indices (T_c) obtained by means of the program MOLDIVS (MOlecular DIversity & Similarity).²²

$$T_c = N(A\&B)/[N(A) + N(B) - N(A\&B)] \quad (5)$$

where $N(A)$ is the number of fragments in molecule A, $N(B)$ is the number of fragments in molecule B, and $N(A\&B)$ is the number of common fragments in molecules A and B.

In this program, molecular fragments are defined as atom centered concentric environments. The fragment consists of a central atom and neighboring atoms connected within a predefined sphere size (the number of bonds between the central and edge atoms). For each atom in a fragment, the information on the atom and bond type, charge, valency, cycle type, and size is coded into fixed-length variables, which are subsequently used to define a pseudorandom hash value for this fragment. The program permits estimation of the similarity of each molecule in the database with all the other molecules by sorting them according to the value of similarity with the initial molecule.

To check the correlation models, all the experimental values were divided in a random way into a training set including 21 compounds and a test set including the other 10 substances (1, 2, 4, 7, 10, 11, 14, 15, 17, 19).

3. RESULTS AND DISCUSSION

3.1. Calcium-Blocking Properties. The results of the ability to inhibit Glu-Ca-uptake ($K_{43/21}$) for the compounds are shown in Table 2.

Table 2. Biological Coefficient Describing Ability to Inhibit Glu-Ca-uptake ($K_{43/21}$), Partition Coefficients n-Octanol/Buffer (pH 7.4) ($D^{oct/buf}$) and n-Hexane/Buffer (pH 7.4) ($D^{hex/buf}$), Apparent Permeability Coefficient (P_{app}) for 1,2,4-Thiadiazole Derivatives

| N | $K_{43/21}$ (%) | $D^{oct/buf}$ | $D^{hex/buf}$ | $10^7 P_{app}$ (cm/s) |
|----|-----------------|---------------|---------------|-----------------------|
| 1 | 84 ± 6 | 149 ± 36 | 0.14 ± 0.04 | 3.36 ± 0.08 |
| 2 | 85 ± 4 | 445 ± 28 | 0.31 ± 0.02 | 3.87 ± 0.19 |
| 3 | 110 ± 10 | 478 ± 16 | 0.12 ± 0.03 | 2.48 ± 0.15 |
| 4 | 75 ± 6 | 226 ± 5 | 0.16 ± 0.04 | 7.47 ± 0.41 |
| 5 | 89 ± 13 | 380 ± 5 | 0.46 ± 0.05 | 8.33 ± 0.23 |
| 6 | 108 ± 8 | 45 ± 1 | 0.14 ± 0.01 | 2.60 ± 0.04 |
| 7 | 66 ± 13 | 560 ± 7 | 0.81 ± 0.05 | 23.7 ± 0.4 |
| 8 | 87 ± 2 | 1038 ± 10 | 1.68 ± 0.07 | 7.6 ± 0.9 |
| 9 | 51 ± 9 | 610 ± 30 | 0.17 ± 0.01 | npm ^a |
| 10 | 88 ± 16 | 316 ± 3 | 0.32 ± 0.02 | 10.7 ± 0.6 |
| 11 | 52 ± 4 | 568 ± 2 | 6.3 ± 0.4 | 94.7 ± 3.6 |
| 12 | 101 ± 14 | 457 ± 2 | 0.36 ± 0.03 | 5.59 ± 0.06 |
| 13 | 108 ± 11 | 205 ± 5 | 0.58 ± 0.03 | 2.48 ± 0.02 |
| 14 | 112 ± 21 | 400 ± 5 | 0.40 ± 0.01 | 7.60 ± 0.16 |
| 15 | 79 ± 13 | 180 ± 10 | 0.115 ± 0.008 | 6.60 ± 0.19 |
| 16 | 86.7 ± 0.5 | 94 ± 13 | 0.48 ± 0.02 | 1.77 ± 0.07 |
| 17 | 47 ± 7 | 1205 ± 10 | 0.80 ± 0.01 | 4.08 ± 0.05 |
| 18 | 30 ± 4 | 250 ± 9 | 1.061 ± 0.012 | 1.30 ± 0.03 |
| 19 | 93 ± 8 | 295 ± 26 | 0.140 ± 0.014 | 2.52 ± 0.19 |
| 20 | 47 ± 6 | 1381 ± 49 | 0.104 ± 0.012 | 2.30 ± 0.01 |
| 21 | 98 ± 10 | 338 ± 6 | 9.0 ± 0.5 | 18.4 ± 0.2 |
| 22 | 87.0 ± 0.6 | 19.2 ± 0.1 | 0.227 ± 0.008 | 6.48 ± 0.77 |
| 23 | 111 ± 2 | 50 ± 3 | 0.42 ± 0.03 | 5.22 ± 0.05 |
| 24 | 86 ± 8 | 145 ± 22 | 16.2 ± 0.1 | 1.08 ± 0.04 |
| 25 | 97 ± 14 | 1.30 ± 0.06 | 0.046 ± 0.003 | 3.85 ± 0.17 |
| 26 | 109 ± 20 | 45 ± 1 | 0.18 ± 0.01 | 12.5 ± 0.2 |
| 27 | 105 ± 6 | 3160 ± 20 | 1.8 ± 0.1 | 14.7 ± 0.9 |
| 28 | 123 ± 4 | 229 ± 6 | 0.13 ± 0.01 | 3.49 ± 0.06 |
| 29 | 121 ± 24 | 90 ± 1 | 0.31 ± 0.02 | 3.21 ± 0.12 |
| 30 | 82 ± 13 | 163 ± 6 | 0.076 ± 0.004 | 8.73 ± 0.02 |
| 31 | 88 ± 4 | 1049 ± 50 | 0.56 ± 0.01 | 2.44 ± 0.03 |

^anpm – not possible to measure.

Several approaches were used to find out the regularity of biological activity ($K_{43/21}$) behavior. First, we tried to disclose the correlations between $\log(K_{43/21})$ and the physicochemical descriptors HYBOT.²¹ Unfortunately, the regularities were not observed. Second, we tried to reveal the correlations of biological activity against the distribution parameters: $\log(D^{oct/buf})$, $\log(D^{hex/buf})$, and $\log(D^{oct/buf}) - \log(D^{hex/buf})$. Our efforts were not successful again. Consequently, we assumed that the interaction of the selected compounds with receptors is not limited by drug delivery processes (absorption, distribution, and others) and is connected directly with the geometry, topology, and nature of the substitutes in the drug molecules. Such observation suggests an idea to analyze the connection of biological activity with the outlined parameters.

In order to carry out a comparative analysis of 1,2,4-thiadiazole phenyl derivatives' biological activity beside the type of the substituent, a separate table (Table 3) was constructed. The diagonal elements of the matrix correspond to monophenyl substituted fragments.

The structure activity relationship of the receptor shows the maximal activity observed for disubstituted phenyl (notably -CH₃ and Cl-) isomers: 2-CH₃-3-Cl- (18) (30%) and 3-CH₃-4-Cl- (17) (47%). On the other hand, the activities of the

Table 3. Biological Coefficient Describing the Ability to Inhibit Glu-Ca-Uptake ($K_{43/21}$, %) for Various Phenyl Substituted 1,2,4-Thiadiazoles

| | | | |
|-------------------|--------------------|--------|-------|
| | 2-Cl | 3-Cl | 4-Cl |
| 2-CH ₃ | n\112 ^a | 30 | |
| 3-CH ₃ | | 101\47 | 47 |
| 4-CH ₃ | | 87 | 85\89 |
| 5-CH ₃ | | 88 | |
| | 2-Cl | 3-Cl | 4-Cl |
| 2-Cl | 112 | | |
| 3-Cl | | 47 | 51 |
| 4-Cl | | | 89 |
| | 2-Cl | 3-Cl | 4-Cl |
| 2-CF ₃ | n\112 | | |
| 3-CF ₃ | | n\47 | |
| 4-CF ₃ | | | 66\89 |
| 5-CF ₃ | 52 | | |
| | 2-Cl | 3-Cl | 4-Cl |
| 2-F | 79\112 | | |
| 3-F | | n\47 | |
| 4-F | | 75 | 88\89 |

^anumber 1\number 2: number 1 corresponds to the activity of i-CH₃-monosubstituted phenyl and number 2 corresponds to the activity of i-Cl-monosubstituted phenyl. n: not measured.

compounds with the same substitutes located at the different positions (3-Cl-4-CH₃- (**8**) and 3-Cl-5-CH₃- (**31**)) are approximately of the same values (88%) (if they are compared to each other), but they are more than twice lower in comparison with the most active substance (**18**). Such an observation indicates strictly the fact that the receptors studied are sensitive to the topology of the selected molecules. It is interesting to note that monophenyl substituted 4-CH₃- (**2**) and 4-Cl- (**5**) have approximately the same activity (89%), which is comparable with the activities of the disubstituted (**8** and **31**) isomers. Thus, the activity of 4-Cl- (**5**) increases essentially when an additional methyl group is introduced into phenyl ring at the meta-position (3-CH₃-4-Cl- (**17**)), and this value becomes comparable with the activity of the mono-Cl-substituted 3-Cl- (**20**) isomer. The above-mentioned approach of molecule structural modification, when the biological activity of the modified molecule is compared with mono-substituted ones, is very useful, as it allows improvement of other characteristics (for example, ADME or membrane permeability) without degradation. As an example, we would like to present the results of Table 2 concerning the apparent coefficients of membrane permeability: for compound **17** this value is twice higher ($4.08 \times 10^{-7} \text{ cm}\cdot\text{s}^{-1}$) in comparison with that of **20** ($2.3 \times 10^{-7} \text{ cm}\cdot\text{s}^{-1}$). Introducing the methyl group at the ortho-position into 3-Cl-substituted phenyl improves the biological activity of the molecule (**17**) (30%), whereas introducing such a substitute into positions 4 (**8**) and 5 (**31**) leads to the degradation of the test property (88%).

Introducing an additional Cl-atom into the most biologically active mono-Cl-isomer (3-Cl- (**20**)) at the para-position (it gives 3-Cl-4-Cl- (**9**)) almost does not change the activity and shows the same effect as the insertion of the methyl group at position 3. Placing the CF₃-group at the para-position of the phenyl ring leads to the maximal increasing of the biological activity (66%) in comparison with the other studied substitutes at this position: CH₃- (85%); OC₂H₅- (110); Cl- (89); OHCHCH₃- (108); F- (88); and OCH₃- (108). In its turn, the biological activity of 2-Cl- (**14**) increases almost twice after

introducing the CF₃-group at the 5-position: this gives 2-Cl-5-CF₃- (**11**) with $K_{43/21} = 52\%$. Moreover, the membrane permeability of the molecule increases by 12 times: $94.7 \times 10^{-7} \text{ cm}\cdot\text{s}^{-1}$ for **11** relative to $7.6 \times 10^{-7} \text{ cm}\cdot\text{s}^{-1}$ for **14**. Thus, we observed the effect of synchronic improvement of both biological activity and membrane permeability. The comparison of Cl- and F-phenyl isomers showed that the 2-F- (**15**) isomer is more active (79%) than 2-Cl- (**14**) (112%). Whereas para-isomers have approximately the same activities: 4-F- (**10**) (88%) and 4-Cl- (**5**) (89%). Introducing an additional F-atom at the para-position of the most active 3-Cl- (**20**) isomer (it gives 3-Cl-4-F- (**4**)) leads to the decrease in the activity from 47 to 75%, respectively.

3.2. Membrane Permeability Properties. The apparent permeability coefficients (P_{app}) of 31 novel 1,2,4-thiadiazoles were measured using the phospholipid membrane approach (Table 2).

As in the previous section, we used HYBOT²¹ descriptors and the conception of the nearest neighbors (with analysis of Tanimoto similarity indices (T_c))²² to find a correlation between P_{app} values and independent variables (the physicochemical descriptors). The analysis of the descriptors demonstrated that the $\log(P_{app})$ function can be described by the descriptor indicating the sum of positive charges on the atoms of the molecule under study ($\sum Q(+)$). The next step was to divide all the experimental data of the training set (21 substances) into clusters including the compounds with Tanimoto similarity indices (T_c) from 0.7 up to 1 for each element of the test set. It should be mentioned that the number of elements in clusters of the compounds selected as a test set differed essentially (from 3 up to 8). The experimental data, entering the cluster, were smoothed by a linear function, because the noted function describes a relationship between the P_{app} value and the $\sum Q(+)$ -descriptor in the best way. After that, the unknown P_{app} value (corresponding to the test set) was estimated by means of the function. Comparative analysis of the predicted and the experimental P_{app} values presented in Figure 1 can be described by the correlation equation:

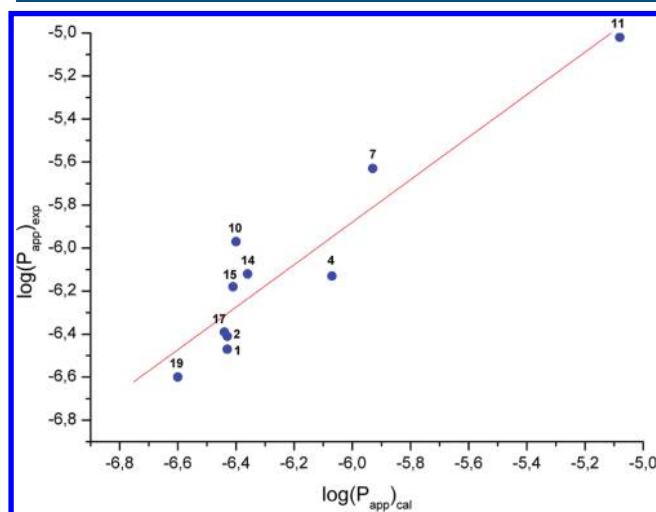


Figure 1. Comparative analysis of the experimental ($\log(P_{app})_{exp}$) versus the predicted ($\log(P_{app})_{cal}$) values for the test set.

$$\log(P_{app})_{exp} = (0.04 \pm 0.82) + (0.99 \pm 0.13) \log(P_{app})_{cal} \quad (6)$$

$$R = 0.934; \sigma = 0.18; n = 10$$

So, knowing only the structural formula of a substance and the number of the nearest physicochemical neighbors in the clusters gives an opportunity to predict the P_{app} value. It should be noted that the training set of P_{app} values includes only 21 compounds (approximately 67% from the total number of studied compounds) and this fact restricts the application capability of the approach, because some clusters have just several structurally similar neighbors. The above-mentioned fact reduces the statistical accuracy of the prognoses. Nevertheless, the available database/set can predict a new P_{app} value safely (as it follows from the test set). It should be noted that if experimental data volume growth persists, the proposed calculation algorithms will work more effectively. In this study we tried to develop a conception of obtaining bioavailable drug molecules on the basis of the available experimental materials. The experiments generating permeability characteristics are going on, and we hope that in the near future calculation procedure precision will be improved essentially.

3.3. Partitioning Properties. **3.3.1. *n*-Octanol/Buffer (pH 7.4) Partitioning.** As the developed class of the compounds is intended for oral introduction, it was interesting to study partition processes taking place at the main types of membranes, which the compounds overcome in order to reach the targets at the cerebral cortex. Immiscible solvent pairs *n*-octanol/buffer (pH 7.4) (describing gastrointestinal tract membranes) and *n*-hexane/buffer (pH 7.4) (characterizing BBB membranes) which are usually used for application purposes were selected as the model systems. We wanted to analyze some correlations/trends between partitioning coefficients, on one hand, and apparent membrane permeability coefficients, on the other hand. For this purpose, the partition coefficients ($D^{oct/buf}$) for 31 novel 1,2,4-thiadiazoles were obtained in the *n*-octanol/buffer (pH 7.4) system (Table 2). As in the previous sections, we used HYBOT descriptors in order to find out the relationships between physicochemical characteristics and partition coefficients. The data analysis showed that the $\log(D^{oct/buf})$ function can be described by the descriptor indicating the sum of H-bond acceptor and donor factors normalized to the polarizability ($\Sigma(C_{ad}/\alpha)$) of the molecule (Figure 2).

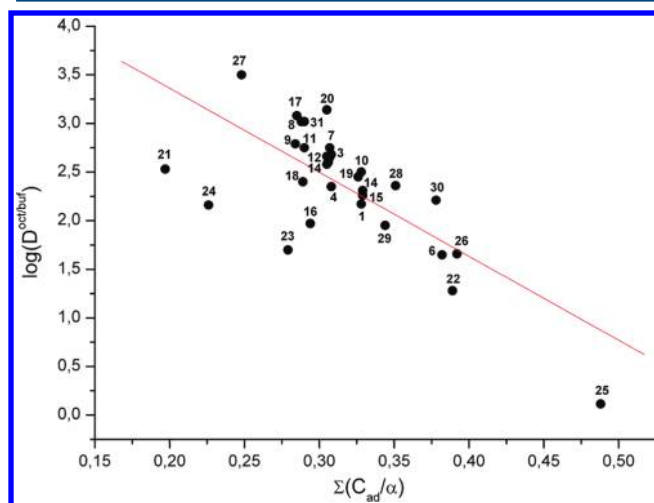


Figure 2. Dependence of $\log(D^{oct/buf})$ versus $\Sigma(C_{ad}/\alpha)$.

$$\log(D^{oct/buf}) = (5.1 \pm 0.5) - (8.6 \pm 1.5) \Sigma(C_{ad}/\alpha) \quad (7)$$

$$R = 0.722; \sigma = 0.45; n = 31$$

It is evident that a low correlation coefficient is observed. Therefore, to improve the model, we used the conception of the nearest neighbors which was also applied in the previous section. For each substance, belonging to the test set, we formed clusters based on the training set with Tanimoto similarity indices from 0.7 up to 1. The $D^{oct/buf}$ value of the test set was estimated from the linear dependence received from a smoothing procedure of the experimental points within the cluster. The results of the calculation are presented in Figure 3 and can be described by the correlation equation:

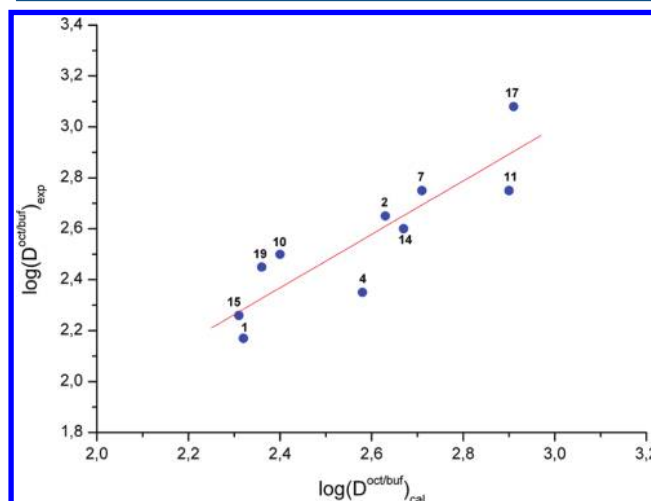


Figure 3. Comparative analysis of the experimental $\log(D^{oct/buf})_{exp}$ versus the predicted $\log(D^{oct/buf})_{cal}$ values for the test set.

$$\log(D^{oct/buf})_{exp} = (-0.1 \pm 0.5) + (1.0 \pm 0.2) \times \log(D^{oct/buf})_{cal} \quad (8)$$

$$R = 0.880; \sigma = 0.14; n = 10$$

The comparison of eqs 7 and 8 shows that the latter model predicts $D^{oct/buf}$ values three times better (if the standard deviation is taken into account) than the former one. Thus, the partition coefficients of this class of the substances can be predicted even if we know their structural formula only. Approximately 90% of the studied 1,2,4-thiadiazoles have $\log(D^{oct/buf})$ values within the range from 1.5 to 3.5. This fact confirms that most of the compounds are lipophilic, and as a consequence, they will prefer lipophilic drug delivery pathways to overcome gastrointestinal tract membranes.

3.3.2. *n*-Hexane/Buffer (pH 7.4) Partitioning. Partition processes in the *n*-hexane/buffer (pH 7.4) system (imitating BBB) were studied in the same way as those in the system described above. For this purpose, the partition coefficients for 31 novel 1,2,4-thiadiazoles were obtained ($D^{hex/buf}$) and the correlations between these values and HYBOT physicochemical descriptors were analyzed. The result of the analysis showed that the experimental values can be described in the best way by the descriptor $\Sigma(C_{ad}/\alpha)$ (Figure 4).

$$\log(D^{hex/buf}) = (2.2 \pm 0.4) - (8.1 \pm 1.2) \Sigma(C_{ad}/\alpha) \quad (9)$$

$$R = 0.771; \sigma = 0.37; n = 31$$

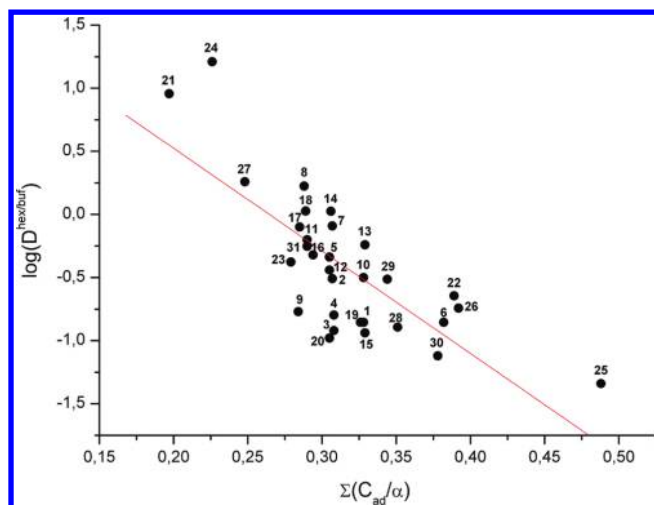


Figure 4. Dependence of $\log(D^{hex/buf})$ versus $\sum(C_{ad}/\alpha)$.

To improve the predictive power of the model, we used the conception of the nearest neighbors explained before.

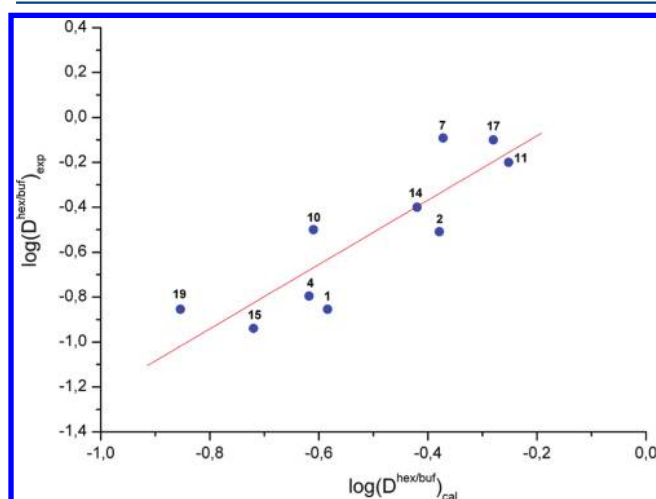


Figure 5. Comparative analysis of the experimental $\log(D^{hex/buf})_{exp}$ versus the predicted $\log(D^{hex/buf})_{cal}$ values for the test set.

The results of the calculations are presented in Figure 5 and can be described by the correlation equation:

$$\log(D^{hex/buf})_{exp} = (0.20 \pm 0.15) + (1.43 \pm 0.28) \log(D^{hex/buf})_{cal} \quad (10)$$

$$R = 0.872; \sigma = 0.17; n = 10$$

The model applying the nn-method predicts $D^{hex/buf}$ values much better in comparison with eq 9. Thus, the partition coefficients of the test substances can be predicted knowing the structural formula only. Approximately 85% of the studied 1,2,4-thiadiazoles have $\log(D^{hex/buf})$ values below 1. This fact confirms that most of the compounds will prefer aqueous drug delivery pathways to overcome the BBB.

Several points should be mentioned about the applicability of the model based on the conception of nearest neighbors. As was shown before, the model using the training set from 21 compounds works well. While a number of substances at the training set increase, the predictive power of the model will

enhance as well. The predictive power of the model for another class of compounds will be determined by the number of structurally relative neighbors at the cluster describing the unknown substance.

3.3.3. Influence of Molecular Topology and Nature of Substituents on Partitioning. As it was said before, the partition coefficients $D^{oct/buf}$ and $D^{hex/buf}$ carry important information about the interactions of drugs with biological barriers (gastrointestinal tract and blood brain barrier in particular). Therefore, it was interesting to analyze the influence of the nature and position of different substitutes in the 1,2,4-thiadiazole phenyl ring on the partition coefficients. Moreover, if we take into account a direct connection of drug delivery to NMDA-subtype and AMPA-subtype receptors with distribution processes in gastrointestinal tract and blood brain barrier blood currents, it becomes very timely to compare the values $D^{oct/buf}$ and $D^{hex/buf}$ and to study the possibilities of changing these values by structural modification of the molecule.

Figure 6 shows distribution coefficient values of 1,2,4-thiadiazole phenyl derivatives in logarithmical coordinates.

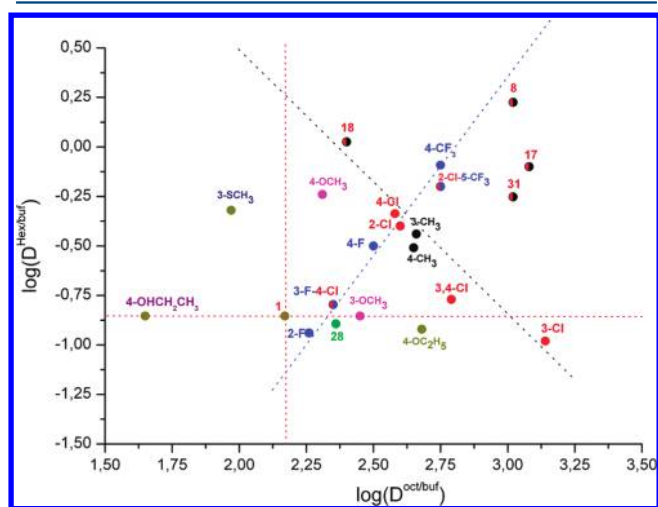


Figure 6. Experimental data in the coordinates $\log(D^{oct/buf})$ versus $\log(D^{hex/buf})$ (numbering corresponds to Table 1).

The red dotted lines, crossing the experimental point that corresponds to unsubstituted phenyl, divide the space into four sectors. Every sector describes the influence of substituents on distribution coefficient values as compared to the case of the unsubstituted molecule. For example, the top right sector corresponds to increasing both $D^{oct/buf}$ and $D^{hex/buf}$ values, etc. This fact means that, for most of the compounds, introduction of substitute to the phenyl ring leads to simultaneously increasing the distribution coefficients under study. The exceptions represent several compounds: 3-SCH₃ (16), for which the decrease of the $D^{oct/buf}$ value and the increase of the $D^{hex/buf}$ value are observed, whereas for 2-F- (15), 3-Cl- (20), 4-OC₂H₅ (3), and (28) the opposite results are revealed: the $D^{oct/buf}$ value grows and $D^{hex/buf}$ falls. It is important that for 4-OHCH₂CH₃ (6) and 3-OCH₃ (19) the $D^{hex/buf}$ value does not grow in comparison with unsubstituted compound, but the $D^{oct/buf}$ value falls for one (6) and grows for one (19).

When studying the position of the substitute in the phenyl ring (isomerism), the following conclusions can be made. The distribution coefficients, $D^{oct/buf}$ and $D^{hex/buf}$, are approximately equal for 2- (14) and 4-Cl (5) isomers. For the meta-isomer

(20), in its turn, a significant increase of the $D^{oct/buf}$ value and a sharp rise for the $D^{hex/buf}$ one are observed. The experimental point corresponding to 3,4-Cl- (9) lies along the straight line connecting the values of the 4-Cl and 3-Cl isomers in the space studied (dotted black line). In other words, the properties of these isomers are additive. The significant difference of the meta-isomer distribution coefficients can be caused by strong conformation changes of the molecule during transfer from one phase to another in comparison with the other isomers. At the same time, it may be such a peculiarity of the meta-isomer that determines partially the abnormally high biological activity ($K_{43/21}$) of phenyl derivate compounds with the Cl-atom in the meta-position: 9, 18, and 4.

The analysis of the available di-isomers Cl- and CH_3 - ($2\text{-CH}_3\text{-3-Cl}$ (18), $3\text{-CH}_3\text{-4-Cl}$ (17), 3-Cl-4-CH_3 (8), and 3-Cl-6-CH_3 (31)) has the following results. For compounds 8, 17, and 31, the $D^{oct/buf}$ values do not differ a lot and are close to the 3-Cl-isomer value. While for compound 18 the distribution coefficient is 1 order of magnitude lower. The $D^{hex/buf}$ values for 8 and 31 have three time differences, while for 17 and 18 the difference is insignificant. The experimental values for methyl isomers 3-CH_3 - (12) and 4-CH_3 - (2) do not differ much from each other and lie along the trend line, connecting Cl- isomers. Moreover, compound $2\text{-CH}_3\text{-3-Cl}$ (18) also lies along this line (Figure 6, black dotted line), which proves the additivity of the properties under consideration for some chlorine- and methyl-isomers.

Such compounds as fluorine isomers (2-F - (15) and 4-F - (10)), 4-CF_3 - (7), as well as disubstituted phenyl with fluorine atoms (3-F-4-Cl - (4) and 2-Cl-5-CF_3 - (11)) lie in the coordinates $\log(D^{oct/buf})$ versus $\log(D^{hex/buf})$ on the trend line (blue dotted line in Figure 6). And the trend lines for chlorine- and fluorine-derivatives differ a lot: they have different inclination angles. Distribution coefficient values rise significantly during the transfer from the 2-F- to 4-F-isomer (for both immiscible phases). Replacing the substitute of fluorine at the para-position with CF_3 - also leads to a significant increase in both the $D^{oct/buf}$ and $D^{hex/buf}$ values. Two trend lines demonstrate that it is possible to change both the lipophilic and hydrophilic properties of the considered class compounds intentionally.

Comparing the properties of 4-CH_3 - (2) and 4-OCH_3 - (13) shows that the introduction of an additional hydrophilic oxygen atom into a substitute results in a decrease of the $D^{oct/buf}$ value and an increase of the $D^{hex/buf}$ value. Adding, in its turn, a methylene group into the methoxy-substitute of 4-OCH_3 - compound (13) (which gives compound $4\text{-OC}_2\text{H}_5$ - (3)) leads to an increase of the $D^{oct/buf}$ value and a significant decrease of the $D^{hex/buf}$ value. It is interesting that placing the methoxy-substitute in the meta-position leads to a considerable decrease of the $D^{hex/buf}$ value and a small rise of the $D^{oct/buf}$ value as compared to the substitution in the para-position. Introducing an oxygen atom into 3-CH_3 - (12) (which gives 3-OCH_3 - (19)) reduces its lipophilicity slightly and decreases the $D^{hex/buf}$ value considerably, whereas a similar introduction of an S-atom into 3-CH_3 - (12) (which gives 3-SCH_3 - (16)) leads to an insignificant change of the $D^{hex/buf}$ value but to a considerable reduction of the $D^{oct/buf}$ value. And finally, a small modification which involves the replacement of substitute $4\text{-OC}_2\text{H}_5$ - (3) with $4\text{-OHCH}_2\text{CH}_3$ - (6) leads to a dramatic decrease of lipophilicity (by an order) while the $D^{hex/buf}$ value remains the same.

3.4. Permeability–Activity Relationship. In order to analyze the relationship between permeability characteristics (P_{app}) and specific biological activity ($K_{43/21}$), the experimental data for the compounds under study were presented in the coordinates $\log(K_{43/21})$ versus $\log(P_{app})$ (Figure 7). All the

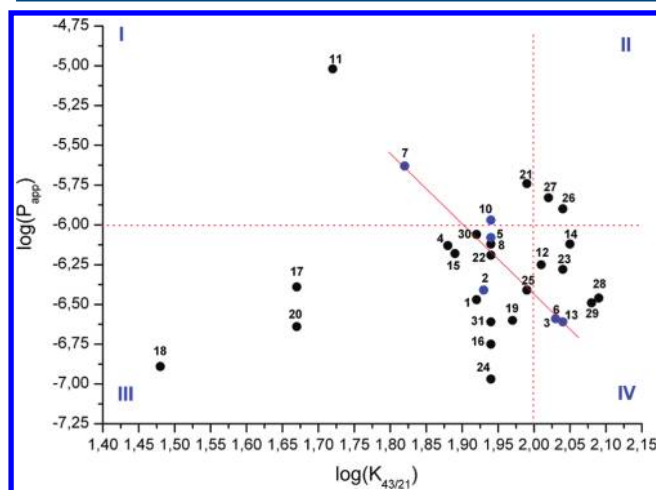


Figure 7. Experimental data in coordinates $\log(P_{app})$ versus $\log(K_{43/21})$ (numbering corresponds to Table 1).

values can be conditionally divided into four groups: (I) with high parameters of permeability (for the considered compounds) and high values of activity (on the tested receptors) ($1 \times 10^{-6} < P_{app}$ ($\text{cm}\cdot\text{s}^{-1}$); $0 < K_{43/21} < 100\%$); (II) with high permeability and low activity ($1 \times 10^{-6} < P_{app}$; $100 < K_{43/21}$); (III) with low permeability and high activity ($P_{app} < 1 \times 10^{-6}$; $0 < K_{43/21} < 100$); (IV) with low permeability and low activity ($P_{app} < 1 \times 10^{-6}$; $100 < K_{43/21}$). The compounds belonging to classes I and III are promising in terms of their further testing. Moreover, the substances of class I are more preferable to those of class III. In their turn, 1,2,4-thiadiazoles of classes II and IV are not suitable for further work and should be structurally modified toward the improvement of the necessary “permeability–activity” properties to replace them with the most favorable group. The most promising “permeability–activity” properties correspond to CF_3 -phenyl derivatives of 1,2,4-thiadiazole (7, 11), which can be recommended as the substances for the further biological and preclinical evaluations/tests.

Comparison of 1,2,4-thiadiazole Cl-phenyl isomers (5, para; 20, meta; 14, ortho) leads to the following conclusions. The permeability characteristics of 5 and 14 are approximately the same; however, the activity values are different: substance 5 belongs to group III, whereas 14 belongs to group IV. Meta-isomer 20 is much more active than the other two ones and for the studied compounds has the minimal $K_{43/2}$ value (together with 17). Nevertheless, the permeability value of the compound is 4 times lower than that of the para- and ortho-isomers. It is difficult to make a decision unambiguously concerning the recommendation for the further testing of substance 20. But if we take into account the maximal biological effect, the compound can be offered for further evaluation.

F-Phenyl isomers of 1,2,4-thiadiazole (10, para; 15, ortho) are situated approximately in the frontier region of groups I and III. This fact confirms insignificant property differences between the compounds. Nevertheless, the para-isomer is

more permeable, whereas the ortho-isomer has better affinity to the biological receptor.

For methylphenyl isomers of 1,2,4-thiadiazole (**2**, para; **12**, meta), the substitution of the meta-isomer with the para-isomer leads to an improvement of biological receptors inhibition, whereas membrane permeability decreases. Compound **12** belongs to class IV, whereas **2** belongs to class III.

For methoxyphenyl isomers of 1,2,4-thiadiazole (**13**, para; **19**, meta), a similar replacement as the one for methyl isomers leads to the opposite effect. The inhibition of the biological receptors becomes worse, whereas the membrane permeability remains approximately the same.

It was interesting to analyze the influence of substitute nature at the para-position of the phenyl ring (blue points) on the “permeability–activity” properties. The results of the analysis are shown in Figure 7 (red line), and the experimental values can be described by the following equation:

$$\log(P_{app}) = (2.4 \pm 1.6) - (4.4 \pm 0.8) \log(K_{43/21}) \quad (11)$$

$$R = 0.9103; \sigma = 0.18; n = 6$$

Thus, it can be assumed that in the future membrane permeability measurements of 1,2,4-thiadiazole para-phenyl derivatives will make it possible to predict $K_{43/21}$ values.

Let us consider the combined impact of two substitutes at the 1,2,4-thiadiazole phenyl ring on the “permeability–activity” properties in comparison with that of mono- derivatives. If we take compound **17** (para-Cl and meta-methyl) and compare it to **5** (para-Cl) and **12** (meta-methyl), the membrane permeability of **17** decreases slightly, whereas the $K_{43/21}$ value decreases anomalously. In the case of comparing substances **4** (para-F and meta-Cl), **10** (para-F), and **20** (meta-Cl), an absolutely opposite effect is observed. The anomalously low $K_{43/21}$ value for **20** (47%) and a high one for **10** (88%) gives the average value for **4** (75%). The analogous regularity (but with the opposite effect) is observed for the membrane permeability data. So, we disclosed the contrary effect of the F- and Cl-substitutes influence on the “permeability–activity” properties.

Thus, the proposed classification of compounds in the space of “permeability–activity” properties allows us to select the most promising substances for their further biological evaluation/testing.

4. CONCLUSIONS

In this study we synthesized and identified novel 1,2,4-thiadiazole derivatives as potent neuroprotectors. The ability to inhibit glutamate stimulated Ca uptake ($K_{43/21}$) was measured. The permeation experiments on phospholipid membranes were carried out, and the apparent permeability coefficients (P_{app}) were obtained. The partition coefficients in *n*-octanol/buffer (pH 7.4) ($D^{oct/buf}$) and *n*-hexane/buffer (pH 7.4) ($D^{hex/buf}$) immiscible phases (as model systems for characterizing gastrointestinal tract membranes and BBB) were determined.

The correlation analysis of $\log(K_{43/21})$ with HYBOT physicochemical descriptors demonstrated that the interaction process between the studied compound and the receptor depends on the specific (C_{ad}) and nonspecific (α) interactions. Moreover, we have proved that the value of biological activity depends considerably on the topology of the molecules under study and the nature of the substitutes in the 1,2,4-thiadiazole phenyl ring. The receptor has such a geometry that the

maximum activity is produced by disubstituted phenyls with substitutes 2-CH₃-3-Cl- (**18**) (30%) and 3-CH₃-4-Cl- (**17**) (47%). On the other hand, the activity of the compounds with the same substitutes 3-Cl-4-CH₃- (**8**) and 3-Cl-5-CH₃- (**31**) is approximately equal (88%) and twice lower in comparison with that of the most active compound (**18**).

We conducted correlation analysis of $\log(D^{oct/buf})$ and $\log(D^{hex/buf})$ with HYBOT physicochemical descriptors by dividing the space into clusters. We received the correlation models that allow us to predict the values in question. Besides, we studied in detail the reciprocal influence of substitutes in the 1,2,4-thiadiazole phenyl ring on the values of the distribution coefficients under study.

The experimental P_{app} values were divided into clusters including the compounds with Tanimoto similarity indices (T_c) lying in the interval from 0.7 up to 1. Within each cluster, P_{app} values can be described by the descriptor indicating the sum of positive charges on the atoms of the studied molecule ($\sum Q(+)$). On the basis of both the received correlation equation and the method of the nearest neighbors, we proposed an algorithm for the prediction of P_{app} values when only the molecular structural formula is known.

We proposed a classification of compounds in the space of the “permeability–activity” properties.

AUTHOR INFORMATION

Corresponding Author

*Institute of Solution Chemistry, Russian Academy of Sciences, 153045 Ivanovo, Russia. Telephone: +7 4932 533784. Fax: +7 4932 336237. E-mail address: glp@isc-ras.ru.

Notes

The authors declare no competing financial interest.

ACKNOWLEDGMENTS

The present research was funded as a part of the basic research program established by the Presidium of the Russian Academy of Sciences “Fundamental sciences for medicine” and the Russian Foundation for Basic Research (No. 09-03-00057).

REFERENCES

- (1) Parsons, C. G.; Danysz, W.; Quack, G. Glutamate in CNS Disorders as a Target for Drug Development: An Update. *Drug News Perspect.* **1998**, *11*, 523–579.
- (2) Nakanishi, N. S. Molecular diversity of glutamate receptors and implications for brain function. *Science* **1992**, *258*, 31–37.
- (3) Dingledine, R.; Borges, K.; Bowie, D.; Traynelis, S. F. The Glutamate receptor ion channels. *Pharmacol. Rev.* **1999**, *51*, 7–61.
- (4) Bräuner-Osborne, H.; Egebjerg, J.; Nielsen, E. Ø.; Madsen, U.; Krosgaard-Larsen, P. Ligands for glutamate receptors: design and therapeutic prospects. *J. Med. Chem.* **2000**, *43*, 2609–2645.
- (5) Petrov, V. I.; Piotrovsky, L. B.; Grigoriev, I. A. *Excitatory Amino Acids*; Volgograd Medical Academy: Volgograd, 1997; p 168.
- (6) Zefirova, O. N.; Zefirov, N. S. Physiologically active compounds acting on glutamate receptors. *Zh. Org. Khim. (Russ.)* **2000**, *36*, 1273–1300.
- (7) Khachaturian, Z. S. Calcium hypothesis of Alzheimer’s disease and brain aging. *Ann. N. Y. Acad. Sci.* **1994**, *747*, 1–11.
- (8) Mattson, M. P.; Cheng, B.; Davis, D.; Bryant, K.; Lieberburg, I.; Rydel, R. E. β -Amyloid peptides destabilize calcium homeostasis and render human cortical neurons vulnerable to excitotoxicity. *J. Neurosci.* **1992**, *12*, 376–389.
- (9) Bleakman, D.; Lodge, D. Neuropharmacology of AMPA and kainate receptors. *Neuropharmacology* **1998**, *37*, 1187–1204.

(10) Siddiquia, N.; Ahuja, P.; Ahsan, W.; Pandey, S. N.; Alam, M. S. Thiadiazoles: Progress Report on Biological Activities. *J. Chem. Pharm. Res.* **2009**, *1* (1), 19–30.

(11) Gupta, A.; Mishra, P.; Pandeya, S. N.; Kashaw, S. K.; Kashaw, V.; Stables, J. P. Synthesis and anticonvulsant activity of some substituted 1,2,4-thiadiazoles. *Eur. J. Med. Chem.* **2009**, *44* (3), 1100–1105.

(12) Lipton, S. A. Paradigm shift in neuroprotection by NMDA receptors blockade: Memantine and beyond. *Nat. Rev. Drug Discovery* **2006**, *5* (2), 160–170.

(13) Nair, N.; Kudo, W.; Smith, M. A.; Abrol, R.; Goddard, W. A. III; Reddy, V. P. Novel purine-based fluoroaryl-1,2,3-triazoles as neuroprotecting agents: Synthesis, neuronal cell culture investigations, and CDK5 docking studies. *Bioorg. Med. Chem. Lett.* **2011**, *21* (13), 3957–3961.

(14) Serkov, I. V.; Proshin, A. N.; Petrova, L. N.; Bachurin, S. O. Novel 1,2,4-thiadiazoles with an NO-producing fragment. *Dokl. Chem.* **2011**, *435* (2), 311–313.

(15) Boulton, J.; Katrizky, A. R.; Hamid, A. M. Heterocyclic rearrangements. Part X. A generalised monocyclic rearrangement. *J. Chem. Soc.* **1967**, 2005–2007.

(16) Macaluso, G.; Cusmano, G.; Buscemi, S. Heterocyclic rearrangements. Rearrangements in the 1,2,4-oxadiazoles, isoxazoles, and 1,2,5-oxadiazoles involving a carbethoxythiourea nitrogen-carbon-sulfur sequence. *Heterocycles* **1986**, *24*, 3433–3439.

(17) Proshin, A. N.; Pushin, A. N.; Makarov, M. V. *Chem. Heterocycl. Compd.* **2007**, *43* (11), 1483–1484.

(18) Perlovich, G. L.; Proshin, A. N.; Volkova, T. V.; Cong, T. B.; Bachurin, S. O. Thermodynamic and structural aspects of novel 1,2,4-thiadiazoles in solid and biological mediums. *Mol. Pharmaceutics* **2011**, *8*, 1807–1820.

(19) Flaten, G. E.; Dhanikula, A. B.; Luthman, K.; Brandl, M. Drug permeability across a phospholipid vesicle-based barrier: a novel approach for studying passive diffusion. *Eur. J. Pharm. Sci.* **2006**, *27*, 80–90.

(20) Artursson, P. Epithelial transport of drugs in cell-culture. I. A model for studying the passive diffusion of drugs over intestinal absorptive (Caco-2) cells. *J. Pharm. Sci.* **1990**, *79*, 476–482.

(21) Raevsky, O. A.; Grigor'ev, V. J.; Trepalin, S. V. HYBOT program package, Registration by Russian State Patent Agency, N 990090 of 26.02.99.

(22) Raevsky, O. A.; Gerasimenko, V. A.; Trepalin, S. V. MOLDIVS (MOLEcular DIVersity & Similarity) program package; Registration by Russian State Patent Agency, N 990093 of 26.02.99.